Title

The Rbm38-p63 feedback loop is critical for tumor suppression and longevity.

Journal

Oncogene, 37(21)

ISSN

0950-9232

Authors

Jiang, Yuqian
Xu, Enshun
Zhang, Jin
et al.

Publication Date

2018-05-01

DOI

10.1038/s41388-018-0176-5

Peer reviewed

HHS Public Access

Author manuscript

Oncogene. Author manuscript; available in PMC 2018 September 09.

Published in final edited form as:

Oncogene. 2018 May ; 37(21): 2863–2872. doi:10.1038/s41388-018-0176-5.

The Rbm38-p63 Feedback Loop Is Critical for Tumor Suppression and Longevity

Yuqian Jiang[1,2], **Enshun Xu**[1,2], **Jin Zhang**[1,2,*], **Mingyi Chen**[3], **Elsa Flores**[4], and **Xinbin Chen**[1,*]

[1]Comparative Oncology Laboratory, University of California at Davis, Davis, CA

[3]Department of Pathology, University of Texas Southwestern Medical Center, Dallas, TX

[4]Department of Molecular Oncology, Moffitt Cancer Center, Tampa, FL

Abstract

The RNA-binding protein Rbm38 is a target of p63 tumor suppressor and can in turn repress p63 expression via mRNA stability. Thus, Rbm38 and p63 form a negative feedback loop. To investigate the biological significance of the Rbm38-p63 loop *in vivo*, a cohort of WT, *Rbm38*$^{-/-}$, *TAp63*$^{+/-}$ and *Rbm38*$^{-/-}$*;TAp63*$^{+/-}$ mice were generated and monitored throughout their lifespan. While mice deficient in *Rbm38* or *TAp63* alone died mostly from spontaneous tumors, compound *Rbm38*$^{-/-}$*;TAp63*$^{+/-}$ mice had an extended lifespan along with reduced tumor incidence. We also found that loss of *Rbm38* markedly decreased the percentage of liver steatosis in *TAp63*$^{+/-}$ mice. Moreover, we found that *Rbm38* deficiency extends the lifespan of tumor-free *TAp63*$^{+/-}$ mice along with reduced expression of senescence-associated biomarkers. Consistent with this, *Rbm38*$^{-/-}$;*TAp63*$^{+/-}$ MEFs were resistant, whereas *Rbm38*$^{-/-}$ or *TAp63*$^{+/-}$ MEFs were prone, to cellular senescence. Importantly, we showed that the levels of inflammatory cytokines (IL17D and Tnfsf15) were significantly reduced *by Rbm38* deficiency in senescence-resistant *Rbm38*$^{-/-}$;*TAp63*$^{+/-}$ mouse livers and MEFs. Together, our data suggest that Rbm38 and p63 function as intergenic suppressors in aging and tumorigenesis and that the Rbm38-p63 loop may be explored for enhancing longevity and cancer management.

Keywords

p63; TAp63; Rbm38; tumorigenesis; SASP; IL17D; Tnfsf15

*Corresponding to jinzhang@ucdavis.edu and xbchen@ucdavis.edu.

[2]Equal contribution

Conflict of Financial Interest: nothing to disclose

Author contribution: Y.J, E.X., and J.Z. performed experiments. Y.J., J.Z., X.C. designed and analyzed the data; E.F. provided the *TAp63*$^{+/-}$ mice. M.C. performed histological analysis. Y.J., J.Z., and X.C. wrote the manuscript.

Introduction

p63 (1, 2), a member of the p53 family, is expressed as two isoforms, TAp63 and ΔNp63, through P1 and P2 promoters, respectively. TAp63 contains an N-terminal activation domain conserved in p53 and regulates an array of genes for tumor suppression (3). In contrast, our previous study showed that ΔNp63 contains a unique activation domain (4, 5), which is distinct from that in TAp63 and consists of 14 unique N-terminal residues and the proline-rich domain. The biological function of p63 has been elucidated in several mouse models. For example, mice deficient in all p63 isoforms show severe development defects, including absence of skin, teeth, mammary gland and limb, and die soon after birth (3, 6). Interestingly, mice deficient in *ΔNp63* isoforms also die soon after birth due to the developmental defects, such as truncated forelimbs and the absence of hind limbs, which largely phenocopies the total *p63*-null mice (7). By contrast, mice deficient in *TAp63* are born alive, but prone to accelerated aging and spontaneous tumors (8, 9). In addition, these mice have defects in lipid metabolism and glucose tolerance (10). Together, these *in vivo* studies indicate a critical role of p63 in skin development, aging, metabolism, and tumorigenesis.

Rbm38, also called RNPC1, is a RNA-binding protein and contains a highly conserved RNA recognition motif (RRM), which consists of two sub-motifs, RNP1 and RNP2. The RRM motif in Rbm38 is found to share a sequence similarity with the ones found in HuR and nucleolin. Previous work from our lab showed that Rbm38 is a target of the p53 family, including p63 (11, 12). Recently, we found that Rbm38 inhibits p63 expression via binding to the p63 3′ untranslated region (3′UTR) and thus, forms a feedback regulatory loop with p63 (13). Interestingly, like *TAp63*-deficient mice (8), we found that *Rbm38*-null mice are prone to premature aging and spontaneous tumors (14). Thus, to investigate the biological significance of the Rbm38-p63 loop in vivo, we generated compound $Rbm38^{-/-};TAp63^{+/-}$ mice and found that these mice had longer lifespan along with reduced tumor incidence as compared to $Rbm38^{-/-}$ or $TAp63^{+/-}$ mice. Furthermore, we found that the decreased susceptibility of compound $Rbm38^{-/-};TAp63^{+/-}$ mice to premature aging and spontaneous tumors is at least in part via decreased senescence-associated secretory phenotype (SASP).

Results

Loss of *Rbm38* extends the lifespan, and reduces the tumor penetrance, in $TAp63^{+/-}$ mice

To make sure that the regulation of p63 by Rbm38 in human cells is conserved in murine cells, we generated a cohort of wild-type, $Rbm38^{-/-}$, $TAp63^{+/-}$, and $Rbm38^{-/-};TAp63^{+/-}$ MEFs. We showed that the level of TAp63 transcripts was increased by loss of *Rbm38* in both wild-type and $TAp63^{+/-}$ MEFs (Fig. 1A). To verify this, $p53^{-/-}$ and $Rbm38^{-/-};p53^{-/-}$ MEFs were generated and confirmed by genotyping (Supplemental Fig. S1A–B). We showed that the level of p63 transcripts was increased in $Rbm38^{-/-};p53^{-/-}$ MEFs as compared to that in $p53^{-/-}$ MEFs (Fig. 1B). These data indicate that the regulation of p63 by Rbm38 is conserved in murine cells and independent of p53, consistent with our previous observation (13).

Rbm38 and p63 form a feedback regulatory loop (13). In addition, mice deficient in *Rbm38* or *TAp63* are prone to spontaneous tumors (8, 14). Thus, examining the role of the Rbm38-p63 loop in tumorigenesis would be instrumental to understand the biological functions of Rbm38 and/or TAp63. To address this, a cohort of wild-type, $Rbm38^{-/-}$, $TAp63^{+/-}$, and $Rbm38^{-/-}$;$TAp63^{+/-}$ mice was generated simultaneously and monitored throughout their lifespan. Both WT and $Rbm38^{-/-}$ mice have been analyzed for another tumor study (14) (Supplemental Table S1–2) and were used as controls for current study. As shown in Fig. 1C, the median lifespan was 121 weeks for WT mice, 102 weeks for $Rbm38^{-/-}$ mice, 101 weeks for $TAp63^{+/-}$ mice, and 113 weeks for $Rbm38^{-/-}$;$TAp63^{+/-}$ mice. Statistical analyses indicated that the median survival time for $Rbm38^{-/-}$ and $TAp63^{+/-}$ mice was significantly shorter than that for WT mice (p=0.0188 for WT vs. $Rbm38^{-/-}$; p=0.000811 for WT vs. $TAp63^{+/-}$). Interestingly, the median survival time for $Rbm38^{-/-}$;$TAp63^{+/-}$ mice was significantly longer than that for $TAp63^{+/-}$ mice (p=0.0310 by LogRank test). Additionally, there was no significant difference in the survival time between WT and $Rbm38^{-/-}$;$TAp63^{+/-}$ mice (p=0.0818 by LogRank test). Next, histology analysis was performed and showed that $TAp63^{+/-}$ and $Rbm38^{-/-}$ mice were prone to spontaneous tumors (Fig. 1D, Table 1, and Supplemental Table S2), consistent with previous reports (8, 14). While $Rbm38^{-/-}$ mice were prone to lymphomas (Fig. 1D and Supplemental Table S1), $TAp63^{+/-}$ mice were prone to both lymphomas and angiosarcomas (Fig. 1D, Table 1, and Supplemental Fig. S1C). Nevertheless, there was no statistical significance in tumor incidence between $Rbm38^{-/-}$ and $TAp63^{+/-}$ mice (p=0.7409 by χ^2 test). Surprisingly, $Rbm38^{-/-}$;$TAp63^{+/-}$ mice were not tumor-prone as compared to $Rbm38^{-/-}$ or $TAp63^{+/-}$ mice (Fig. 1D, Table 1–2, and Supplemental Table S2). The difference in the tumor incidence was statistically significant between $Rbm38^{-/-}$;$TAp63^{+/-}$ and $Rbm38^{-/-}$ (p=0.0387 by χ^2 test) as well as betwen $Rbm38^{-/-}$;$TAp63^{+/-}$ and $TAp63^{+/-}$ mice (p=0.02 by χ^2 test). Additionally, there was no statistical difference in the tumor incidence between WT and $Rbm38^{-/-}$;$TAp63^{+/-}$ mice (p=0.7966 by χ^2 test). Together, these results suggest that the *Rbm38* deficiency extends the lifespan and reduces tumor penetrance in $TAp63^{+/-}$ mice.

Rbm38 deficiency reduces the incidence of liver steatosis in $TAp63^{+/-}$ mice

TAp63 plays a role in lipid metabolism and as a result, mice deficient in *TAp63* are prone to liver steatosis (fatty liver disease) (10), a process of abnormal retention of lipids in liver cells. Thus, liver tissues of $TAp63^{+/-}$, and $Rbm38^{-/-}$;$TAp63^{+/-}$ mice along with WT and $Rbm38^{-/-}$ mice were examined for liver steatosis. Although WT and $Rbm38^{-/-}$ mice were analyzed for a previous tumor study (14), liver steatosis was not examined in these mice. We found that all four groups of mice developed liver steatosis (Fig. 2A), which is characterized by the large vacuoles or “bubbles” as fat solves during tissue processing. Interestingly, the percentage of liver steatosis was low in WT (17.65%) and $Rbm38^{-/-}$ (8.7%) mice, but high in $TAp63^{+/-}$ (52.38%) mice (Fig. 2B). Surprisingly, we found that *Rbm38* deficiency markedly decreased the incidence of liver steatosis from 52.38% in $TAp63^{+/-}$ mice to only 13.63% in $Rbm38^{-/-}$;$TAp63^{+/-}$ mice (Fig. 2B). Pairwise comparison indicated that the difference in liver steatosis was significant between WT and $TAp63^{+/-}$ mice (p=0.0273 by χ^2 test), between $Rbm38^{-/-}$ and $TAp63^{+/-}$ mice (p=0.0015 by χ^2 test), and between $Rbm38^{-/-}$;$TAp63^{+/-}$ and $TAp63^{+/-}$ mice (p=0.0154 by χ^2 test). By contrast, there was no significant difference in liver steatosis between WT and $Rbm38^{-/-}$ mice (p=0.3974 by χ^2

test), between WT and *Rbm38*$^{-/-}$;*TAp63*$^{+/-}$ mice (p=0.8813 by χ^2 test), and between *Rbm38*$^{-/-}$ and *Rbm38*$^{-/-}$;*TAp63*$^{+/-}$ mice (p=0.4798 by χ^2 test). Together, these data suggest that *Rbm38* deficiency ameliorates liver steatosis in *TAp63*$^{+/-}$ mice.

Loss of *Rbm38* alleviates aging-related phenotypes in *TAp63*$^{+/-}$ mice

Previous studies indicate that mice deficient in *TAp63* or *Rbm38* exhibited aging-related phenotypes such as shorter lifespan and reduced body fat (9, 14). Thus, to determine the role of the Rbm38-p63 loop in accelerated aging, the lifespan of tumor-free *TAp63*$^{+/-}$, *Rbm38*$^{-/-}$, and *Rbm38*$^{-/-}$;*TAp63*$^{+/-}$ mice were plotted. Interestingly, we found that the median lifespan was 101 weeks for *TAp63*$^{+/-}$ mice, 94 weeks for *Rbm38*$^{-/-}$ mice, and 108 weeks for *Rbm38*$^{-/-}$;*TAp63*$^{+/-}$ mice (Fig. 3A and supplemental Fig. S2A–B). The difference in lifespan between *Rbm38*$^{-/-}$;*TAp63*$^{+/-}$ and *TAp63*$^{+/-}$ mice was statistically significant (p=0.039 by LogRank test) (Fig. 3A). However, there was no significant difference in the lifespan between *Rbm38*$^{-/-}$;*TAp63*$^{+/-}$ and *Rbm38*$^{-/-}$ mice (p=0.138 by LogRank test) (Supplemental Fig. S2A) or between *TAp63*$^{+/-}$ and *Rbm38*$^{-/-}$ mice (p=0.728 by LogRank test) (Supplemental Fig. S2B). Next, the activity of senescence associated-β-galactosidase (SA-β-gal), a widely used biomarker for aging (15, 16), was examined in the liver tissues of gender-matched WT, *Rbm38*$^{-/-}$, *TAp63*$^{+/-}$, and *Rbm38*$^{-/-}$;*TAp63*$^{+/-}$ mice at age of around 83 weeks (Fig. 3B). The WT and *Rbm38*$^{-/-}$ mice were generated from a previous study (Supplemental Tables S1–2) (14). We found that the SA-β-gal activity was enhanced in *Rbm38*$^{-/-}$ and *TAp63*$^{+/-}$ livers as compared to that in WT livers (Fig. 3B). Importantly, in *Rbm38*$^{-/-}$;*TAp63*$^{+/-}$ livers, the SA-β-gal activity was markedly reduced when compared to that in *Rbm38*$^{-/-}$ and *TAp63*$^{+/-}$ livers but was similar to that in WT livers (Fig. 3B). Similar observations were found in another set of age- and gender-matched WT, *Rbm38*$^{-/-}$, *TAp63*$^{+/-}$, and *Rbm38*$^{-/-}$;*TAp63*$^{+/-}$ mice (Supplemental Fig. S3A). We also showed that the SA-β-gal activity was reduced in the liver and kidney tissues of a *Rbm38*$^{-/-}$;*TAp63*$^{+/-}$ mouse as compared to *TAp63*$^{+/-}$ mouse (Supplemental Fig. S3B). Furthermore, the level of p16^{Ink4a} transcript, an aging biomarker (17, 18), was examined in liver tissues of WT, *Rbm38*$^{-/-}$, *TAp63*$^{+/-}$, and *Rbm38*$^{-/-}$;*TAp63*$^{+/-}$ mice at age of around 83 weeks (Fig. 3C) or 124 (Fig. 3D) weeks. We showed that *Rbm38* deficiency led to an increase in TAp63 transcript in *Rbm38*$^{-/-}$ and *Rbm38*$^{-/-}$;*TAp63*$^{+/-}$ liver tissues (Fig. 3C), consistent with previous observations (13) (Fig. 1A). Notably, compared to WT livers, the level of p16^{Ink4a} transcript was increased in the *Rbm38*$^{-/-}$ and *TAp63*$^{+/-}$ livers, but unchanged or slightly decreased in *Rbm38*$^{-/-}$;*TAp63*$^{+/-}$ livers (Fig. 3C–D, p16^{Ink4a} panels). Similarly, we showed that the level of liver p16^{Ink4a} transcripts in a *Rbm38*$^{-/-}$;*TAp63*$^{+/-}$ mouse was lower than that in a *TAp63*$^{+/-}$ mouse (Supplemental Fig. 3C). Together, these data suggest that *Rbm38* deficiency alleviates aging-related phenotypes in *TAp63*$^{+/-}$ mice.

Loss of *Rbm38* reduces cellular senescence in *TAp63* heterozygous MEFs and liver tissues

Cellular senescence serves as an important tumor-suppressor mechanism by preventing the proliferation of premalignant cells (19, 20). Interestingly, recent studies suggest that cellular senescence serves as a double-edged sword in promoting aging and cancer as senescent cells secrets many proinflammatory cytokines, a process called SASP (21, 22). Thus, SA-β-gal assay was performed in WT, *Rbm38*$^{-/-}$, *TAp63*$^{+/-}$, and *Rbm38*$^{-/-}$;*TAp63*$^{+/-}$ MEFs. We

found that the percentage of SA-β-gal-positive cells was markedly increased in *Rbm38*$^{-/-}$ MEFs (20%) and *TAp63*$^{+/-}$ MEFs (25%) as compared to that in wild-type MEFs (10%) (Fig. 4A–B). Importantly, SA-β-positive cells were markedly reduced by loss of *Rbm38* from 25% in *TAp63*$^{+/-}$ MEFs to 13% in *Rbm38*$^{-/-}$;*TAp63*$^{+/-}$ MEFs, which was statistically significant ($p<0.05$) (Fig. 4A–B). Previously, we showed that *Rbm38* deficiency leads to cellular senescence (23) along with increased expression of IL17D and Tnfsf15 (14). IL17D, a member of IL17 family, and Tnfsf15, a member of a member of the tumor necrosis factor (TNF) ligand superfamily, are proinflammatory cytokines (24, 25) and likely involved in SASP. Thus, RT-PCR was performed to measure the levels of IL17D and Tnfsf15 in WT, *Rbm38*$^{-/-}$, *TAp63*$^{+/-}$ and *Rbm38*$^{-/-}$;*TAp63*$^{+/-}$ MEFs. As a control, we measured the level of TAp63 transcript and showed that *Rbm38* deficiency led to an increase in TAp63 transcript in *Rbm38*$^{-/-}$ and *Rbm38*$^{-/-}$;*TAp63*$^{+/-}$ MEFs (Fig. 4C), consistent with a previous report (13). Similarly, the levels of IL17D and Tnfsf15 were increased in *Rbm38*$^{-/-}$ MEFs (Fig. 4C), consistent with a previous report (14). Interestingly, we found that the levels of IL17D and Tnfsf15 transcripts were also increased in *TAp63*$^{+/-}$ MEFs as compared to that in wild-type MEFs (Fig. 4C). However, the levels of IL17D and Tnfsf15 were reduced by *Rbm38* deficiency in *Rbm38*$^{-/-}$;*TAp63*$^{+/-}$ MEFs (Fig. 4B). To further test this, the levels of IL17D and Tnfsf15 transcripts were examined in the liver tissues of WT, *Rbm38*$^{-/-}$, *TAp63*$^{+/-}$, and *Rbm38*$^{-/-}$;*TAp63*$^{+/-}$ mice at age of around 83 weeks (Fig. 4D) or 124 weeks (Fig. 4E). We found that the levels of IL17D and Tnfsf15 transcripts were increased in the *Rbm38*$^{-/-}$ and *TAp63*$^{+/-}$ liver tissues as compare to WT liver tissues (Fig. 4D–E). By contrast, in *Rbm38*$^{-/-}$;*TAp63*$^{+/-}$ livers, the level of IL17D and Tnfsf15 transcripts was similar to that in WT liver tissues, but much lower than that in *Rbm38*$^{-/-}$ and *TAp63*$^{+/-}$ liver tissues (Fig, 4D–E). Together, these data suggest that the Rbm38-p63 loop modulates tumor suppression and premature aging potentially via SASP.

Discussion

We showed previously that Rbm38 and p63 mutually regulate each other and forms a feedback loop (11, 13). Thus, to investigate the Rbm38-p63 loop *in vivo*, a cohort of WT, *Rbm38*$^{-/-}$, *TAp63*$^{+/-}$, *Rbm38*$^{-/-}$;*TAp63*$^{+/-}$ mice was generated and monitored for aging and spontaneous tumors. Interestingly, we found that compared with *Rbm38*$^{-/-}$ or *TAp63*$^{+/-}$ mice, compound *Rbm38*$^{-/-}$;*TAp63*$^{+/-}$ mice had a longer lifespan and decreased susceptibility to spontaneous tumors and liver steatosis (Figs. 1–2). We also showed that cellular senescence, a key mediator of aging and cancer, was alleviated by loss of *Rbm38* in *Rbm38*$^{-/-}$;*TAp63*$^{+/-}$ MEFs and tissues. Furthermore, the levels of proinflammatory cytokines (IL17D and Tnfsf15) were markedly decreased by loss of *Rbm38*, thus relieving the burden of inflammation in *Rbm38*$^{-/-}$;*TAp63*$^{+/-}$ mice. Based on these findings, a model for the role of the Rbm38-p63 loop in longevity and tumor suppression is proposed and shown in Fig. 4F.

Here, we found that *Rbm38*$^{-/-}$;*TAp63*$^{+/-}$ mice exhibited significant improvements in longevity and tumor suppression as compared to *TAp63*$^{+/-}$ mice, (Fig. 1C–D). Similarly, the median survival time for tumor-free *Rbm38*$^{-/-}$;*TAp63*$^{+/-}$ mice was significantly longer than that for *TAp63*$^{+/-}$ mice (Fig. 3A). These data suggest that the aging and tumorigenesis mediated by *TAp63* deficiency can be ameliorated by *Rbm38* deficiency, representing a

phenomenon called “intergenic suppression”. Thus, to explore how TAp63 and Rbm38 act as intergenic suppressors in aging and tumorigenesis, three possibilities merit further investigation: (1) the increased level of TAp63 in *Rbm38*$^{-/-}$;*TAp63*$^{+/-}$ mice (Figs. 1A–B, 3C–D, and 4C–E) may contribute to the longer lifespan and reduced tumor penetrance; (2) loss of *Rbm38* may alter a pathway that compensates for the TAp63 pathway in tumor suppression and premature aging; (3) IL17D and Tnfsf15 are suppressed by combined loss of *Rbm38* and *TAp63* (Fig. 4C–E), which subsequently reduces the burden of inflammation necessary for aging and tumor promotion.

In this study, we also found that the percentage of mice with liver steatosis was significantly reduced in *Rbm38*$^{-/-}$;*TAp63*$^{+/-}$ mice as compared to that in *TAp63*$^{+/-}$ mice (Fig. 2B). We postulate that the increased expression of TAp63 by *Rbm38* deficiency may be responsible for the decreased liver steatosis in compound *Rbm38*$^{-/-}$;*TAp63*$^{+/-}$ mice (Fig. 1A–B). Indeed, TAp63 is a major regulator in lipid metabolism as *TAp63*-deficient mice become obese and prone to liver steatosis (10). However, a recent study indicated that activation of TAp63 promotes, whereas down-regulation of TAp63 inhibits, liver steatosis via IKKβ/ER stress in a p53-deficient mouse model (26). Another possibility is probably due to the reduction of adipose tissue induced by *Rbm38* deficiency (14), which would be independent of p63. Thus, further studies are needed to determine how the Rbm38-p63 loop regulates lipid metabolism by using conditional *Rbm38*- and/or *TAp63*-deficient mouse models.

Cellular senescence has been considered as a potent tumor-suppressive mechanism by inducing growth arrest of malignant cells (27, 28). However, recent studies suggest that senescent cells can secret proinflammatory cytokiens, which would change the tissue microenvironment and promote tumorigenesis (21, 29). Based on these observations, it is hypothesized that cellular senescence suppresses tumor initiation but promotes tumor progression (30). In our study, we found that cellular senescence and two proinflammatory cytokines (IL17D and Tnfsf15) were reduced in *Rbm38*$^{-/-}$;*TAp63*$^{+/-}$ MEFs and tissues as compared to that in *Rbm38*$^{-/-}$ or *TAp63*$^{+/-}$ MEFs and tissues (Figs. 3–4). Interestingly, IL17D can stimulate the production of IL6 and IL8, both of which are critical SASP factors (31). Additionally, Tnfsf15 is known to activate NF-kappaB, which is a key regulator of SASP (32). Thus, our results suggest that SASP is alleviated by loss of *Rbm38*, leading to the extended lifespan and reduced tumor penetrance in *Rbm38*$^{-/-}$;*TAp63*$^{+/-}$ mice. However, it is not clear how Rbm38 and/or TAp63 control IL17D and Tnfsf15 expression. Additionally, it is not clear how IL17D and Tnfsf15 are involved in TAp63- and/or Rbm38-mediated longevity and tumor suppression. The answers to these questions would help us better understand the biological significance of the Rbm38-p63 loop in tumor suppression and premature aging.

Materials and Methods

Mice

Rbm38-conditional knockout mice (on a pure C57BL/6 background) were previously generated as described in (23). The *TAp63*$^{+/-}$ mice (on a C57BL/6 background) were previously generated by Dr. Elsa Flores’ laboratory (9). *Rbm38*$^{-/-}$; *TAp63*$^{+/-}$ mutant mice were generated by intercrossing *Rbm38*$^{+/-}$ with *Rbm38*$^{+/-}$; *TAp63*$^{+/-}$ mice. All animals and

use protocols were approved by the University of California at Davis Institutional Animal Care and Use Committee.

MEF isolation

To isolate WT, *Rbm38*$^{-/-}$, *TAp63*$^{+/-}$, and *Rbm38*$^{-/-}$; *TAp63*$^{+/-}$ MEFs, *Rbm38*$^{+/-}$;*TAp63*$^{+/-}$ mice were bred with *Rbm38*$^{+/-}$;*TAp63*$^{+/-}$ mice. At 13.5-day, embryos were isolated as described previously (33). The MEFs were cultured in DMEM supplemented with 10% FBS (HyClone), 55 μM β-mercaptoethanol, and 1× non-essential amino acids (NEAA) solution (Cellgro).

RNA Isolation and RT-PCR Analysis

The RT-PCR analysis was performed as previously described (34). Briefly, total RNA was isolated and then subjected to cDNA synthesis using RevertAid Reverse transcriptase (Fisher). The PCR program used for amplification was (i) 95 °C for 5 min, (ii) 95 °C for 1 min, (iii) 58 °C for 1min, (iv) 72 °C for 1 min, and (v) 72 °C for 10 min. From steps ii–iv, the cycle was repeated 22 times for actin or GAPDH, 30 times for Rbm38 and TAp63, 35 times for IL17D, Tnfsf15 and p16. The primers for mouse TAp63 were a forward primer, 5′-TAG AGA TCT GCC ATG TCG CA-3′, and a reverse primer, 5′-GCA TGC GGA TAC AAT CCA TG-3′. The primers for Rbm38, actin, IL17D, Tnfsf15, GAPDH, and p16 were the same as the ones described previously (14).

SA-β-Gal Staining

The senescence assay was performed as described previously (35). Briefly, primary MEFs at passage 4 were harvested, fixed, and stained with X-gal overnight at 37°C. The percentage of SA-β-gal-positive cells was calculated as the ratio of SA-β-gal-positive cells versus total cells. Total 150 cells were counted in triplicates. For SA-β-Gal staining in tissues, tissues were fixed with 2% (vol/vol) formaldehyde and 0.2% glutaraldehyde for 20 min at room temperature, followed by staining with fresh β-gal staining solution overnight at 37 °C. The tissues were processed, embedded with paraffin, counterstained with nuclear fast red.

Histological Analysis

The histological assay was performed as previously described (14). Briefly, mouse tissues were fixed with formalin for 18 hour, followed by embedding process in paraffin blocks. Tissue sections (6 μm) were sectioned and stained with Hematoxylin and eosin. All the mouse tissues were blindly reviewer by a pathologist without knowing the mouse genotypes.

Statistical Analysis

The LogRank Test was used for determination of the differences in survival of different genotypes. χ^2 test was used for comparison between tumor incidence or liver steatosis from different genotypes. Student t-test was used to determine the statistical significance of SA-β-gal staining assay. A p value that is smaller than 0.05 was considered significant.

Supplementary Material

Refer to Web version on PubMed Central for supplementary material.

Acknowledgments

This work is supported in part by National Institutes of Health (CA195828 to Chen, XB).

References

1. Yang A, McKeon F. P63 and P73: P53 mimics, menaces and more. Nat Rev Mol Cell Biol. 2000; 1(3):199–207. [PubMed: 11252895]
2. Yang A, Kaghad M, Caput D, McKeon F. On the shoulders of giants: p63, p73 and the rise of p53. Trends Genet. 2002; 18(2):90–5. [PubMed: 11818141]
3. Yang A, Kaghad M, Wang Y, Gillett E, Fleming MD, Dotsch V, et al. p63, a p53 homolog at 3q27-29, encodes multiple products with transactivating, death-inducing, and dominant-negative activities. Mol Cell. 1998; 2(3):305–16. [PubMed: 9774969]
4. Harms K, Nozell S, Chen X. The common and distinct target genes of the p53 family transcription factors. Cell Mol Life Sci. 2004; 61(7–8):822–42. [PubMed: 15095006]
5. Dohn M, Zhang S, Chen X. p63alpha and DeltaNp63alpha can induce cell cycle arrest and apoptosis and differentially regulate p53 target genes. Oncogene. 2001; 20(25):3193–205. [PubMed: 11423969]
6. Mills AA, Zheng B, Wang XJ, Vogel H, Roop DR, Bradley A. p63 is a p53 homologue required for limb and epidermal morphogenesis. Nature. 1999; 398(6729):708–13. [PubMed: 10227293]
7. Romano RA, Smalley K, Magraw C, Serna VA, Kurita T, Raghavan S, et al. DeltaNp63 knockout mice reveal its indispensable role as a master regulator of epithelial development and differentiation. Development. 2012; 139(4):772–82. [PubMed: 22274697]
8. Su X, Chakravarti D, Cho MS, Liu L, Gi YJ, Lin YL, et al. TAp63 suppresses metastasis through coordinate regulation of Dicer and miRNAs. Nature. 2010; 467(7318):986–90. [PubMed: 20962848]
9. Su X, Paris M, Gi YJ, Tsai KY, Cho MS, Lin YL, et al. TAp63 prevents premature aging by promoting adult stem cell maintenance. Cell Stem Cell. 2009; 5(1):64–75. [PubMed: 19570515]
10. Su X, Gi YJ, Chakravarti D, Chan IL, Zhang A, Xia X, et al. TAp63 is a master transcriptional regulator of lipid and glucose metabolism. Cell Metab. 2012; 16(4):511–25. [PubMed: 23040072]
11. Shu L, Yan W, Chen X. RNPC1, an RNA-binding protein and a target of the p53 family, is required for maintaining the stability of the basal and stress-induced p21 transcript. Genes Dev. 2006; 20(21):2961–72. [PubMed: 17050675]
12. Chen X, Liu G, Zhu J, Jiang J, Nozell S, Willis A. Isolation and characterization of fourteen novel putative and nine known target genes of the p53 family. Cancer Biol Ther. 2003; 2(1):55–62. [PubMed: 12673118]
13. Zhang J, Jun Cho S, Chen X. RNPC1, an RNA-binding protein and a target of the p53 family, regulates p63 expression through mRNA stability. Proc Natl Acad Sci U S A. 2010; 107(21):9614–9. [PubMed: 20457941]
14. Zhang J, Xu E, Ren C, Yan W, Zhang M, Chen M, et al. Mice deficient in Rbm38, a target of the p53 family, are susceptible to accelerated aging and spontaneous tumors. Proc Natl Acad Sci U S A. 2014; 111(52):18637–42. [PubMed: 25512531]
15. Gary RK, Kindell SM. Quantitative assay of senescence-associated beta-galactosidase activity in mammalian cell extracts. Anal Biochem. 2005; 343(2):329–34. [PubMed: 16004951]
16. Itahana K, Campisi J, Dimri GP. Methods to detect biomarkers of cellular senescence: the senescence-associated beta-galactosidase assay. Methods Mol Biol. 2007; 371:21–31. [PubMed: 17634571]
17. Hall BM, Balan V, Gleiberman AS, Strom E, Krasnov P, Virtuoso LP, et al. Aging of mice is associated with p16(Ink4a)- and beta-galactosidase-positive macrophage accumulation that can be induced in young mice by senescent cells. Aging (Albany NY). 2016; 8(7):1294–315. [PubMed: 27391570]
18. Krishnamurthy J, Torrice C, Ramsey MR, Kovalev GI, Al-Regaiey K, Su L, et al. Ink4a/Arf expression is a biomarker of aging. J Clin Invest. 2004; 114(9):1299–307. [PubMed: 15520862]

19. Collado M, Blasco MA, Serrano M. Cellular senescence in cancer and aging. Cell. 2007; 130(2): 223–33. [PubMed: 17662938]
20. Campisi J. Cancer, aging and cellular senescence. In Vivo. 2000; 14(1):183–8. [PubMed: 10757076]
21. Coppe JP, Desprez PY, Krtolica A, Campisi J. The senescence-associated secretory phenotype: the dark side of tumor suppression. Annu Rev Pathol. 2010; 5:99–118. [PubMed: 20078217]
22. Freund A, Orjalo AV, Desprez PY, Campisi J. Inflammatory networks during cellular senescence: causes and consequences. Trends Mol Med. 2010; 16(5):238–46. [PubMed: 20444648]
23. Zhang J, Cho SJ, Shu L, Yan W, Guerrero T, Kent M, et al. Translational repression of p53 by RNPC1, a p53 target overexpressed in lymphomas. Genes Dev. 2011; 25(14):1528–43. [PubMed: 21764855]
24. Pappu R, Ramirez-Carrozzi V, Sambandam A. The interleukin-17 cytokine family: critical players in host defence and inflammatory diseases. Immunology. 2011; 134(1):8–16. [PubMed: 21726218]
25. Meylan F, Richard AC, Siegel RM. TL1A and DR3, a TNF family ligand-receptor pair that promotes lymphocyte costimulation, mucosal hyperplasia, and autoimmune inflammation. Immunol Rev. 2011; 244(1):188–96. [PubMed: 22017439]
26. Porteiro B, Fondevila MF, Delgado TC, Iglesias C, Imbernon M, Iruzubieta P, et al. Hepatic p63 regulates steatosis via IKKbeta/ER stress. Nat Commun. 2017; 8:15111. [PubMed: 28480888]
27. Narita M, Lowe SW. Senescence comes of age. Nat Med. 2005; 11(9):920–2. [PubMed: 16145569]
28. Braig M, Lee S, Loddenkemper C, Rudolph C, Peters AH, Schlegelberger B, et al. Oncogene-induced senescence as an initial barrier in lymphoma development. Nature. 2005; 436(7051):660–5. [PubMed: 16079837]
29. Coppe JP, Patil CK, Rodier F, Sun Y, Munoz DP, Goldstein J, et al. Senescence-associated secretory phenotypes reveal cell-nonautonomous functions of oncogenic RAS and the p53 tumor suppressor. PLoS Biol. 2008; 6(12):2853–68. [PubMed: 19053174]
30. Campisi J, d'Adda di Fagagna F. Cellular senescence: when bad things happen to good cells. Nat Rev Mol Cell Biol. 2007; 8(9):729–40. [PubMed: 17667954]
31. Hwang SY, Kim JY, Kim KW, Park MK, Moon Y, Kim WU, et al. IL-17 induces production of IL-6 and IL-8 in rheumatoid arthritis synovial fibroblasts via NF-kappaB- and PI3-kinase/Akt-dependent pathways. Arthritis Res Ther. 2004; 6(2):R120–8. [PubMed: 15059275]
32. Wen L, Zhuang L, Luo X, Wei P. TL1A-induced NF-kappaB activation and c-IAP2 production prevent DR3-mediated apoptosis in TF-1 cells. J Biol Chem. 2003; 278(40):39251–8. [PubMed: 12882979]
33. Scoumanne A, Cho SJ, Zhang J, Chen X. The cyclin-dependent kinase inhibitor p21 is regulated by RNA-binding protein PCBP4 via mRNA stability. Nucleic Acids Res. 2011; 39(1):213–24. [PubMed: 20817677]
34. Zhang J, Yan W, Chen X. p53 is required for nerve growth factor-mediated differentiation of PC12 cells via regulation of TrkA levels. Cell Death Differ. 2006; 13(12):2118–28. [PubMed: 16729028]
35. Qian Y, Zhang J, Yan B, Chen X. DEC1, a basic helix-loop-helix transcription factor and a novel target gene of the p53 family, mediates p53-dependent premature senescence. J Biol Chem. 2008; 283(5):2896–905. [PubMed: 18025081]

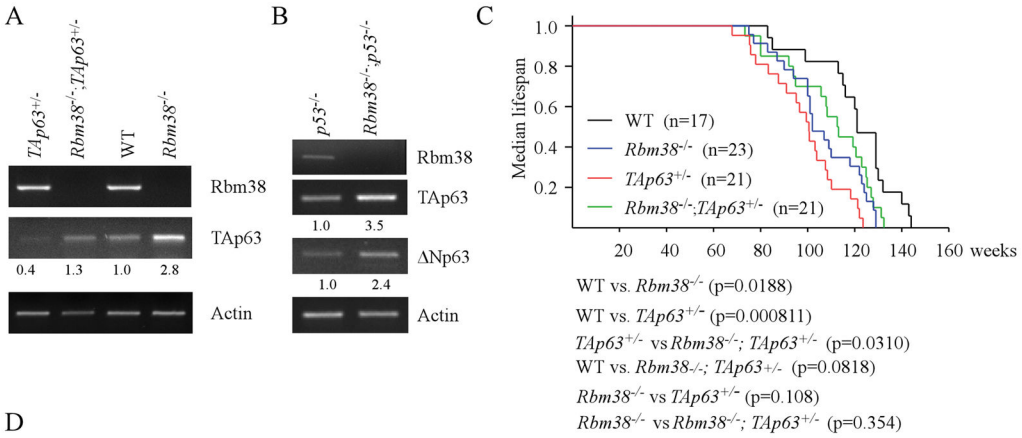

D

Tumor spectrum	WT# (n=17)	*Rbm38*$^{-/-}$# (n=23)	*TAp63*$^{+/-}$ (n=21)	*Rbm38*$^{-/-}$; *TAp63*$^{+/-}$ (n=19)*
Lymphoma	2	8	5	3
Hepatoma	0	4	0	0
Hemangioma	0	0	1	0
Adenocarcinoma	0	0	0	1
Angiosarcoma	0	2	7	1
Liposarcoma	0	0	1	0
Histiocyticsarcoma	1	1	0	0
Total tumors	3	15	14	5
Tumor-bearing mice	3/17	12/23	12/21	4/19

data was adapted from *PNAS*, 111(52):18637-42.
* Two mice were found dead and excluded from the tumor study
Differences in tumor incidence: WT vs *Rbm38*$^{-/-}$ (p=0.0258); WT vs *TAp63*$^{+/-}$ (p= 0.0133); WT vs *Rbm38*$^{-/-}$; *TAp63*$^{+/-}$ (p=0.7966); *Rbm38*$^{-/-}$ vs *TAp63*$^{+/-}$ (p=0.7409) *Rbm38*$^{-/-}$ vs *Rbm38*$^{-/-}$; *TAp63*$^{+/-}$ (p=0.0387); *TAp63*$^{+/-}$ vs *Rbm38*$^{-/-}$;*TAp63*$^{+/-}$ (p = 0.02).

Figure 1. Loss of *Rbm38* extends the lifespan, and reduces the tumor penetrance, in *TAp63*$^{+/-}$ mice

(A) The level of Rbm38, TAp63, and actin was determined in WT, *Rbm38*$^{-/-}$, *TAp63*$^{+/-}$, and *Rbm38*$^{-/-}$; *TAp63*$^{+/-}$ MEFs. The level of TAp63 transcripts was normalized to that of actin and arbitrarily set at 1.0 in WT MEFs. The relative -fold change of each protein level is shown below each lane. The data are representative of three independent experiments. (B) The level of Rbm38, TAp63, ΔNp63, and actin was determined in *p53*$^{-/-}$ and *Rbm38*$^{-/-}$;*p53*$^{-/-}$ MEFs. (C) Kaplan-Meier survival curves of WT (n=17), *Rbm38*$^{-/-}$ (n=23), *TAp63*$^{+/-}$ (n=21), and *Rbm38*$^{-/-}$;*TAp63*$^{+/-}$ (n=21) mice. The median survival time is 121 weeks for WT mice, 102 weeks for *Rbm38*$^{-/-}$ mice, 101 weeks for *TAp63*$^{+/-}$ mice, and 113 weeks for *Rbm38*$^{-/-}$;*TAp63*$^{+/-}$ mice. (D) The tumor spectrum in WT (n =17), *Rbm38*$^{-/-}$ (n=23), *TAp63*$^{+/-}$ (n=21), and *Rbm38*$^{-/-}$;*TAp63*$^{+/-}$ (n=19) mice.

A

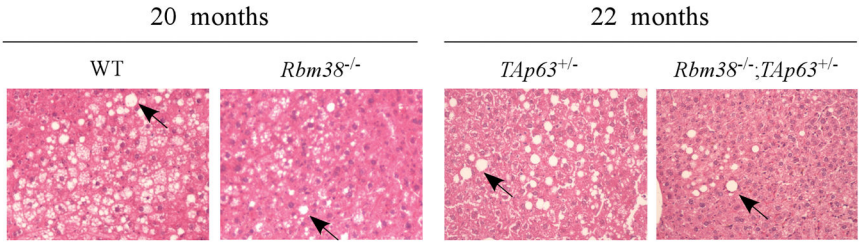

B

Genotype	Fatty liver	Percentage of fatty liver
WT (n=17)	3	17.65%
Rbm38$^{-/-}$ (n=23)	2	8.70%
TAp63$^{+/-}$ (n=21)	11	52.38%
Rbm38$^{-/-}$; *TAp63*$^{+/-}$ (n=19)	3	13.63%

Differences in fatty liver : WT vs. *Rbm38*$^{-/-}$ (p = 0.3974)
WT vs *TAp63*$^{+/-}$ (p=0.0273)
WT vs *Rbm38*$^{-/-}$;*TAp63*$^{+/-}$ (p=0.8813)
Rbm38$^{-/-}$ vs *TAp63*$^{+/-}$ (p=0.0015)
Rbm38$^{-/-}$ vs *Rbm38*$^{-/-}$;*TAp63*$^{+/-}$ (p=0.4798)
TAp63$^{+/-}$ vs. *Rbm38*$^{-/-}$;*TAp63*$^{+/-}$ (p = 0.0154)

Figure 2. *Rbm38* deficiency reduces the incidence of liver steatosis in *TAp63*$^{+/-}$ mice

(A) H&E stained liver sections from WT, *Rbm38*$^{-/-}$, *TAp63*$^{+/-}$, and *Rbm38*$^{-/-}$;*TAp63*$^{+/-}$ mice at age of 20–22 months. Arrows indicate the liver steatosis in the liver tissues characterized as large vacuoles in the liver tissue. (B) The percentage of liver steatosis in WT (n=17), *Rbm38*$^{-/-}$ (n=23), *TAp63*$^{+/-}$ (n=21), and *Rbm38*$^{-/-}$;*TAp63*$^{+/-}$ (n=19) mice.

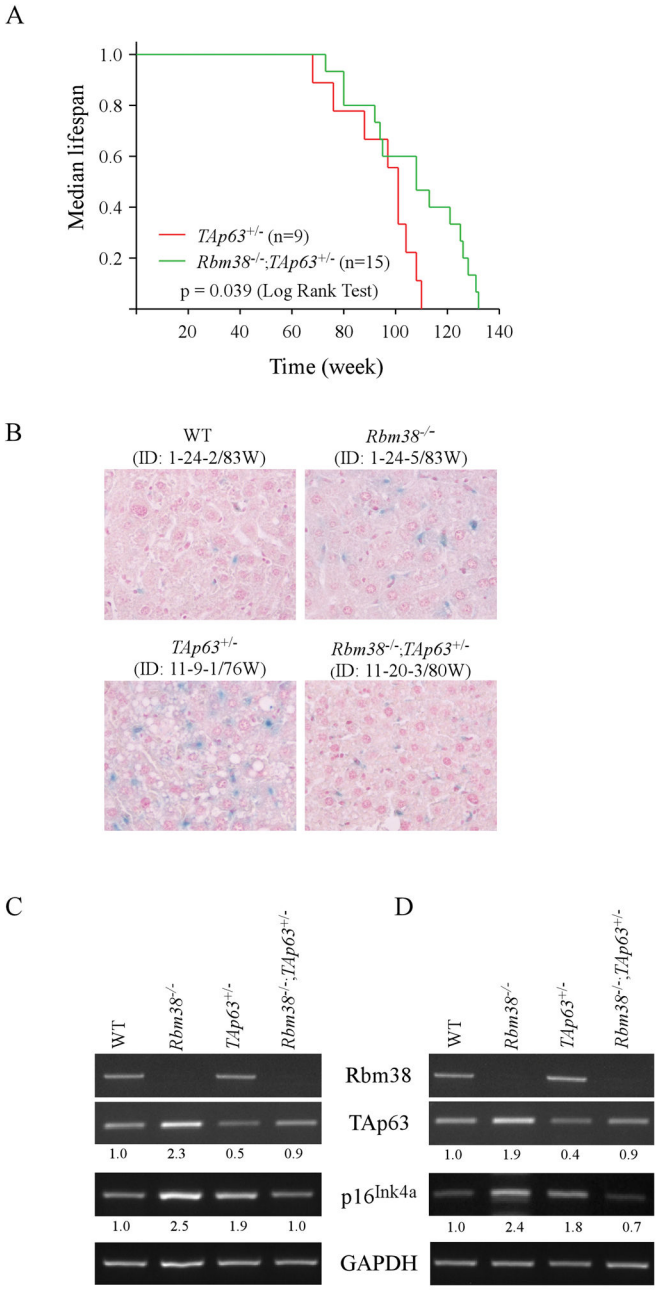

Figure 3. Loss of *Rbm38* alleviates aging-related phenotypes in *TAp63*$^{+/-}$ mice

(A) Kaplan-Meier survival curves of tumor-free *TAp63*$^{+/-}$ (n=9) and *Rbm38*$^{-/-}$;*TAp63*$^{+/-}$ (n=15) mice. The median survival time is 101 weeks for *TAp63*$^{+/-}$ mice and 108 weeks for *Rbm38*$^{-/-}$;*TAp63*$^{+/-}$ mice (p=0.039 by LogRank test). (B) The SA-β-gal-stained liver tissues of WT (ID: 1-24-2/83W), *Rbm38*$^{-/-}$ (ID:1-24-5/83W), *TAp63*$^{+/-}$ (ID: 11-9-1/76W), and *Rbm38*$^{-/-}$;*TAp63*$^{+/-}$ (ID: 11-20-3/80W) were sectioned and counterstained with nuclear fast red. (D) The level of Rbm38, TAp63, p16^{Ink4A} and GAPDH was determined in the liver tissues from WT (ID: 1-24-2/83W), *Rbm38*$^{-/-}$ (ID:1-24-5/83W), *TAp63*$^{+/-}$ (ID: 2-13-6/68W) and *Rbm38*$^{-/-}$;*TAp63*$^{+/-}$ (ID:11-2-2/83W) mice. (E) The level of Rbm38,

TAp63, $p16^{Ink4A}$ and GAPDH was determined in the liver tissues from WT (ID: 3-9-7/128W), *Rbm38*$^{-/-}$ (ID: 11-16-14/129W), *TAp63*$^{+/-}$ (ID: 2-13-1/113W) and *Rbm38*$^{-/-}$;*TAp63*$^{+/-}$ (ID:11-26-4/124W) mice.

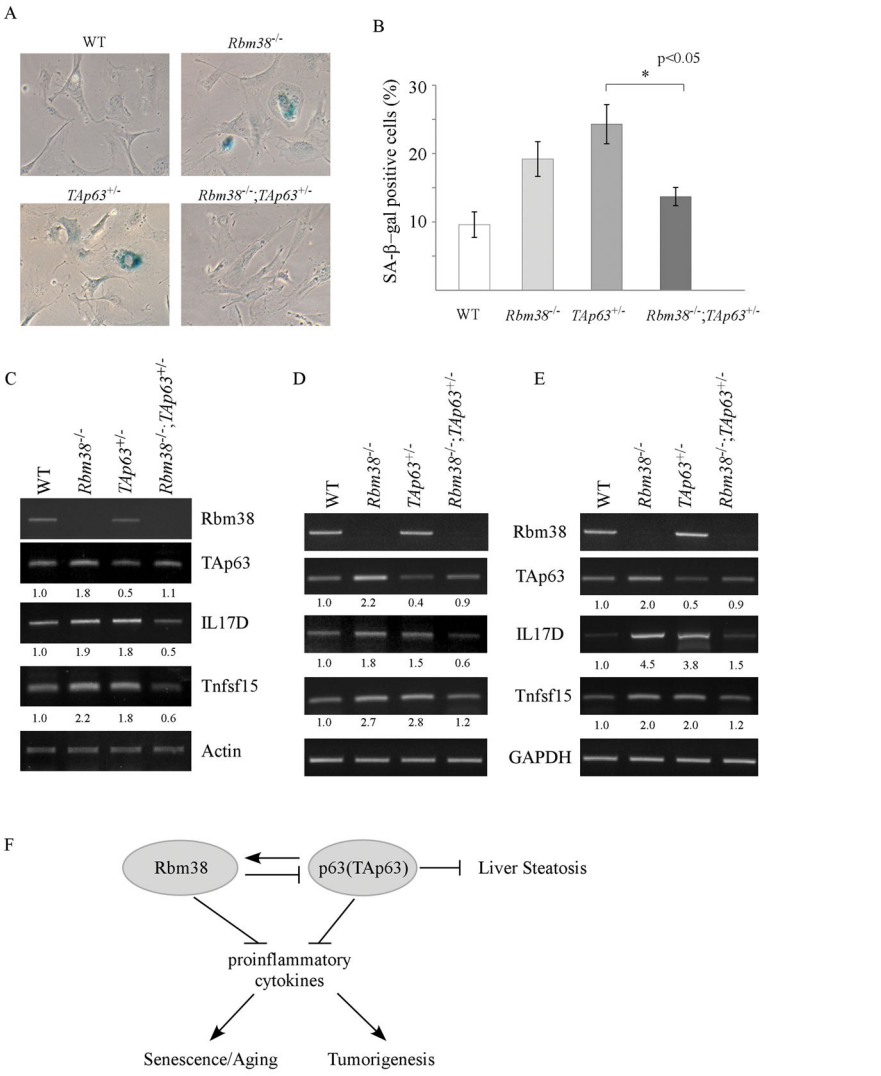

Figure 4. Loss of *Rbm38* significantly reduces cellular senescence in *TAp63* heterozygous MEFs and liver tissues

(A) Primary WT, *Rbm38*$^{-/-}$, *TAp63*$^{+/-}$ and *Rbm38*$^{-/-}$;*TAp63*$^{+/-}$ MEFs at passage 4 were used for SA-β-gal assay as described in the Materials and Methods. (B) Quantification of the percentage of SA- β-gal-positive cells shown in (A). (C) The level of Rbm38, TAp63, IL17D, Tnfsf15 and actin was determined in WT, *Rbm38*$^{-/-}$, *TAp63*$^{+/-}$, and *Rbm38*$^{-/-}$;*TAp63*$^{+/-}$ MEFs. (D) The level of IL17D, Tnfsf15 and GAPDH was determined in the liver tissues from WT (ID: 1-24-2/83W), *Rbm38*$^{-/-}$ (ID: 1-24-5/83W), *TAp63*$^{+/-}$ (ID: 2-13-6/68W) and *Rbm38*$^{-/-}$;*TAp63*$^{+/-}$ (ID:11-2-2/83W) mice. (E) The level of IL17D, Tnfsf15 and GAPDH was determined in the liver tissues from WT (ID: 3-9-7/128W), *Rbm38*$^{-/-}$ (ID: 11-16-14/129W), *TAp63*$^{+/-}$ (ID: 2-13-1/113W) and *Rbm38*$^{-/-}$;*TAp63*$^{+/-}$ (ID:11-26-4/124W) mice. (F) A proposed model for the role of Rbm38-p63 loop in inflammation, aging and tumorigenesis.

Table 1

Survival time and tumor spectrum in TAp63+/− mice (n=21)

ID	Gender	Survival (Week)	Tumor	Liver Steatosis	Other abnormalities
11	F	78	hemangioma	Yes	None
13	M	121	angiosarcoma	Yes	EMH, interstitial nephritis
14	M	99	lymphoma; angiosarcoma	No	EMH, interstitial nephritis
16	M	124	angiosarcoma	No	spleen with white pulp hyperplasia
17	M	103	B-cell lymphoma; angiosarcoma	No	interstitial nephritis
25	M	118	angiosarcoma	No	spleen with red pulp hyperplasia
28	M	95	liposarcoma	Yes	interstitial nephritis
5	F	108	lymphoma	No	interstitial nephritis
3	F	122	lymphoma	No	spleen with white pulp hyperplasia, interstitial nephritis
1-20-1	M	91	angiosarcoma	Yes	red pulp hemorrhage
10-2-1	M	83	lymphoma	Yes	red pulp hemorrhage
11-15-2	F	75	hemangiosarcoma	Yes	white pulp hyperplasia, glomerulosclerosis
19	F	97	No	No	interstitial nephritis
10	M	88	No	No	interstitial nephritis
10-2-4	M	110	No	Yes	red pulp hemorrhage
3-2-15	F	108	No	Yes	EMH, white pulp hyperplasia
21	M	101	No	No	penomonia, interstitial nephritis, glomerulosclerosis
11-15-3	M	104	No	Yes	None
11-19-1	M	76	No	Yes	None
2-13-6	F	68	No	No	None
27	M	101	No	Yes	None
				Used for experiments below	
2-13-6	M	68		Fig. 3C–D, Fig. 4D–E	
2-13-1	M	113		Fig. 3C–D, Fig. 4D–E	
24	M	120		Supplemental Fig. S3A	

EMH: extramedullary hematopoiesis

Table 2

Survival time and tumor spectrum in Rbm38−/−; TAp63+/− mice (n=21)

ID	Gender	Survival (week)	Tumor	Liver steatosis	Other abnormalities
8-17-3	M	127	lymphoma	No	Red pulp hemorrhage in spleen
8-19-9	F	125	lymphoma	No	Interstitial nephritis
8-19-8	M	113	hemangiosarcoma, adenocarcinoma	Yes	None
10-6-2	F	106	lymphoma	Yes	None
5-1-12	M	128	No	No	None
5-1-6	M	108	No	No	None
6-15-9	M	132	No	No	None
8-11-3	F	94	No	Yes	EMH
8-15-1	M	113	No	No	None
11-20-3	M	80	No	No	Red pulp hemorrhage in spleen, interstitial nephritis
5-4-4	F	80	No	No	White pulp hyperplasia in spleen
10-21-6	M	131	No	No	None
11-23-2	M	126	No	No	None
11-26-4	M	121	No	No	Red pulp hemorrhage in spleen
11-28-6	M	95	No	No	None
5-1-3	M	92	No	No	None
7-28-5	F	73	No	No	Liver ballooning degeneration
8-11-4	M	125	No	No	None
11-2-4	M	108	No	No	None
8-20-4	M	123	N/A	N/A	Found dead
10-2-5	M	119	N/A	N/A	Found dead
				Used for experiments below	
11-2-2	M	83		Fig. 3C–D, Fig. 4D–E	
11-26-4	M	113		Fig. 3C–D, Fig. 4D–E	
5-1-3	M	92		Supplemental Fig. S3B	

EMH: extramedullary hematopoiesis